JES
JOURNAL OF ENVIRONMENTAL SCIENCES
ISSN 1001-0742
CN 11-2629/X
May 1, 2013 Volume 25 Number 5
www.jesc.ac.cn

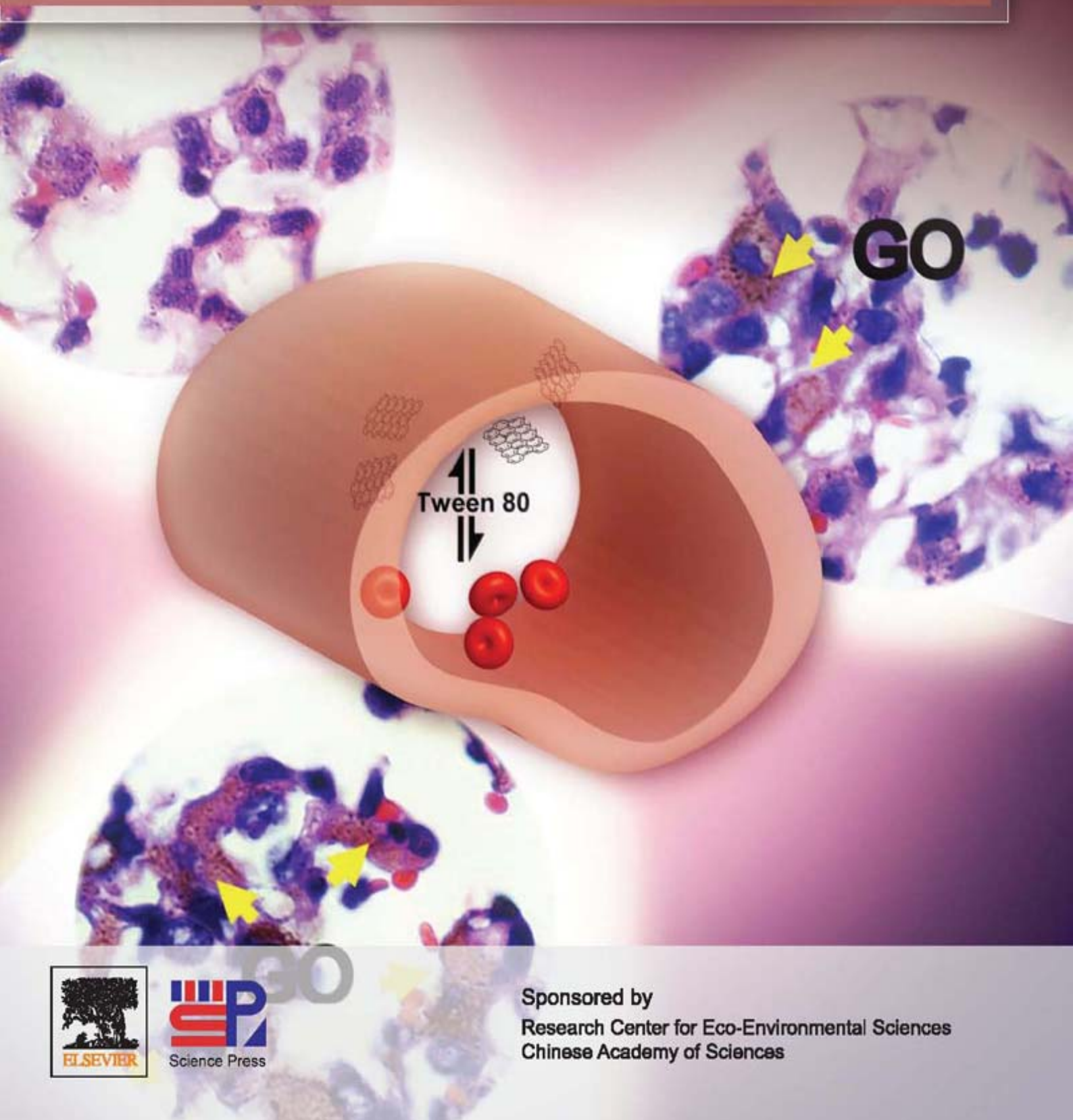

ELSEVIER
Science Press
Sponsored by
Research Center for Eco-Environmental Sciences
Chinese Academy of Sciences

ISSN 1001–0742 **Journal of Environmental Sciences** Vol. 25 No. 5 2013

CONTENTS

Environmental biology

Environmental health and toxicology

Atmospheric environment

Aquatic environment

Environmental catalysis and materials

Serial parameter: CN 11-2629/X*1989*m*205*en*P*24*2013-5

Available online at www.sciencedirect.com
ScienceDirect
Journal of Environmental Sciences 2013, 25(5) 1034–1043
JOURNAL OF ENVIRONMENTAL SCIENCES
ISSN 1001-0742
CN 11-2629/X
www.jesc.ac.cn

Photo-catalytic decolourisation of toxic dye with N-doped titania: A case study with Acid Blue 25

Dhruba Chakrabortty*, Susmita Sen Gupta

Department of Chemistry, B N College, Dhubri, Assam, India

Received 07 July 2012; revised 04 September 2012; accepted 18 September 2012

Abstract

Dyes are one of the hazardous water pollutants. Toxic Acid Blue 25, an anthraquinonic dye, has been decolourised by photo-catalysing it with nitrogen doped titania in aqueous medium. The photo catalyst was prepared from 15% $TiCl_3$ and 25% aqueous NH_3 solution as precursor. XRD and TEM revealed the formation of well crystalline anatase phase having particle size in the nano-range. BET surface area of the sample was higher than that of pure anatase TiO_2. DRS showed higher absorption of radiation in visible range compared to pure anatase TiO_2. XPS revealed the presence of nitrogen in N-Ti-O environment. The experimental parameters, namely, photocatalyst dose, initial dye concentration as well as solution pH influence the decolourisation process. At pH 3.0, the N-TiO_2 could decolourise almost 100% Acid Blue 25 within one hour. The influence of N-TiO_2 dose, initial concentration of Acid Blue 25 and solution pH on adsorption-desorption equilibrium is also studied. The adsorption process follows Lagergren first order kinetics while the modified Langmuir-Hinselwood model is suitably fitted for photocatalytic decolourisation of Acid Blue 25.

Key words: Acid Blue 25; decolourisation; nitrogen-doped titania; photocatalysis

DOI: 10.1016/S1001-0742(12)60108-9

Introduction

Dyes are widely used in textile, leather, paper, plastic, and other industries. These are synthetic aromatic compounds containing various functional groups. The wastewater that spiked with dyes are aesthetically displeasing and also hinders the light penetration into the stream and thus results in the destruction of the aquatic ecosystem (Fu et al., 2011). Some dyes can cause allergy, dermatitis, skin irritation, mutations, and cancer in humans (Bhatnagar et al., 2009). Anthraquinonic dyes represent the second most important class of commercial dyes after azo-compounds and are mainly used for dyeing wool, polyamide and leather (Ghodbane and Hamdaoui, 2009). One of the noticeable anthraquinoic dye is Acid Blue 25, that causes skin, eye irritation and may also create respiratory problem. Thus the decontamination of this dye is major concern to the environmentalists.

Among different physical and chemical methods, heterogeneous photocatalysis assisted by various semiconductors has been considered as a cost-effective and alternative treatment process for the purification of dye-containing wastewater.

* Corresponding author. E-mail: chakraborttydhruba@gmail.com

TiO_2 is considered to be the most promising photocatalyst because of its high efficiency, low cost, chemical intentness and photo-stability (Burda et al., 2003). But, due to wide band gap (3.2 eV), ultraviolet irradiation is required for photocatalytic activation of TiO_2. It is not possible to use solar radiation efficiently using TiO_2 as photocatalyst because ultra violet radiation accounts for only about 5% of the solar radiation. In addition the high rate of electron-hole recombination on the surface and in the bulk phase of the catalyst as well as low photo-electric conversion efficiency are the hindrances for the practical applicability of TiO_2 as photocatalyst. So to make TiO_2 an effective catalyst for visible light photocatalysis some modifications are to be carried out.

One of the widely used modification methods is doping with noble and transition metals (Kemp and Mclntyre, 2006; Du et al., 2008; Li et al., 2008; Sobana et al., 2008; He et al., 2010; Liu et al., 2011). However metal doping can result in thermal instability and increase in carrier trapping, which may decrease the photo catalytic efficiency (Zhu et al., 2006; Cong et al., 2007). Non-metal doping has been found to be effective to extend the photo response of TiO_2 into visible region (Sato et al., 2005; Yu et al., 2005; Cong et al., 2007). Various non metals such as B, C, N, S, F, I etc. are used for the purpose (Tachikawa et

al., 2004; Xu et al., 2008; Ao et al., 2009; Bidaye et al., 2009; Wang and Lim, 2010; Ma et al., 2011; Wu et al, 2011). Besides, particle size also plays important role in determining the efficiency of the photocatalyst (Narayan et al., 2009). In order to maximise the photocatalytic activity, the catalyst particles should be small enough to offer higher number of active sites per unit mass. Thus the synthesis of photocatalyst in nano range has been tried as a method of modification (Zhang et al., 1998).

Asahi et al. (2001) first reported that N-doping could reduce the band gap of TiO_2 and improve its photocatalytic activity in the visible region. N-doping is widely used for developing visible light responsive TiO_2 photocatalyst for its effectiveness in narrowing the band gap (Liu et al., 2009). There are several methods for N-doping, some of which are physical methods like ion implantation (Ghicov et al., 2006; Livraghi et al., 2006), magnetron sputtering (Mwabora et al., 2004), chemical vapour deposition (Chen and Burda, 2004; Valentin et al., 2005), while the others are chemical methods, like, solvothermal process (Gandhe and Fernandes, 2005), sol-gel synthesis (Sakthivel et al., 2004; Sathish et al., 2005), chemical treatment of TiO_2 (Irie et al., 2003; Diwald et al., 2004), oxidation of titanium nitride (Livraghi et al., 2006), etc. Various titanium compounds like $Ti(OCH(CH_3)_2)_4$ (Wang et al., 2007), $Ti(OBu)_4$ (Wang et al., 2009), $TiCl_4$ (Li et al., 2009), $TiCl_3$ (Yin et al., 2005). TiO_2 (Irie et al., 2003; Silveyra et al., 2005) etc. have been used as the source of titanium. Many kinds of nitrogen sources are used as doping agent, which include urea, triethyl amine, ammonia, ammonium chloride, ammonium nitrates, hydrazine and so on (Livraghi et al., 2006; Chi et al., 2007; Cong et al., 2007; Xing et al., 2009).

In this work, nano sized ($\leq$ 10 nm) TiO_2 has been synthesized using $TiCl_3$ and aqueous NH_3. The material has been found to be quite active for photochemical decolourisation of Acid Blue 25 under visible light irradiation.

1 Experimental

1.1 Materials

$TiCl_3$ (15%, LobaChemie) and 25% NH_3 solution (E Merck) are used as source of titanium and nitrogen respectively. The TiO_2 (anatase) was procured from Alfa Aesar. Acid Blue 25 [1-amino-9,10-dihydro-9,10-dioxo-4-(phenylamino)-2-anthracenesulfonic acid, monosodium salt] (C.I. number: 62055, molecular formula: $C_{20}H_{13}N_2NaO_5S$) was procured from Sigma-Aldrich and is used without further purification.

1.2 Preparation of the catalyst

A 150-mL of $TiCl_3$ was taken in a Teflon beaker and 100 mL aqueous NH_3 solution was added drop wise with constant stirring at 353 K. The process took about 2 hr, after which the mixture was stirred for an additional period of 1 hr. The colour of the mixture first changed to blue and then became brownish yellow. The pH of the resulting mixture was 6.5. The solid precipitate was separated and washed with distilled water for several times and finally dried in air oven at 343 K. The sample was then calcined at 623 K for 4 hr in a muffle furnace to get a yellowish brown powder.

1.3 Characterization methods

The X-ray powder diffraction patterns of the samples are recorded on a Rigaku Miniflex diffractometer using nickle-filtered Cu $K\alpha$ radiation. The BET surface area of the catalysts has been measured by nitrogen adsorption method at 77 K with the help of Quantachrome Autosorb-1C surface area analyzer, using BET equation. The TEM investigation of the samples are carried out with JEOL JEM 2100 instrument operating at an accelerating voltage of 200 kV. The XPS investigation was done on ThermoScientific ESCALAB 250 instrument with monochromatized Al X-ray source. Diffuse reflectance UV-Visible spectra of the samples were obtained using a HITACHI-400 spectrophotometer.

1.4 Determination of adsorption efficiency

The adsorption experiments has been carried out in 100 mL Erlenmeyer flasks by mixing together a constant amount of catalyst dose with a constant volume of the aqueous dye solution. The contents in the flasks were agitated by placing them in a constant temperature water bath thermostat shaker for a known time interval under dark. The mixture was then centrifuged (Remi R 24) and concentration of dye solution remaining unadsorbed in the supernatant liquid has been determined with spectrometer (Elico SL 177, India) at λ_{max} 600 nm. The adsorption parameters, namely, the influence of catalyst load (0.25 to 1.50 g/L), initial dye concentration (18.0 to 36.0 μmol/L) and pH (3.0 to 11.0) were studied.

1.5 Determination of photocatalytic activity

The catalytic reaction was carried out in a glass reactor having water circulation facility. A 250-W halogen bulb is used as the source of visible light fitted with a glass filter to cut-off short wavelengths (λ < 420 nm). In a typical reaction 200 mL (18 μmol/L) of the dye solution is taken with requisite amount of the catalyst and kept in dark for 60 min under stirring to attain the adsorption-desorption equilibrium. The mixture is then exposed to visible light under constant string with the help of a magnetic stirrer. The concentration of dye after adsorption (60 min) is considered as the initial concentration for photocatalytic study. Eloquent is collected at a regular interval and the concentration of the dye is measured with the help of spectrometer as before.

2 Result and discussion

2.1 Photocatalyst characterization

Figure 1 shows X-ray powder diffraction pattern of the N-TiO_2 sample which reveals formation of highly crystalline anatase titania. From the diffraction pattern, the presence of any other phase is ruled out. The particle size of N-TiO_2 has been calculated from the (101) peak with the help of Scherrer equation (Lin et al., 2002; Cong et al., 2007):

$$D = k\lambda/\beta\cos\theta \quad (1)$$

where, $k = 0.9$, $\lambda = 0.154$ nm, β = full width half maxima and θ = diffraction angle. The calculated value of the particle size of N-TiO_2 and TiO_2 was approximately 6.2 and 12 nm, respectively.

The diffused reflectance spectra of N-TiO_2 and TiO_2 are shown in **Fig. 2**. It can be seen that the visible light absorption is higher in the case of N-TiO_2 and it extends to about 600 nm. The band gap energy (E_g) was calculated on the basis of the equation $E_g = 1240/\lambda$ (Shao et al., 2008), λ (nm) is the wavelength value corresponding to the point of intersection between the vertical and the horizontal line in the spectra. The band gap energy for TiO_2 was found to be 3.17 eV. On the other hand in N-TiO_2, there are two band gap at 2.87 and 2.01 eV. The former band gap should be due to TiO_2 environment while the later one must have resulted from N-doping. There is red shift of minimum 0.3 eV in the N-TiO_2 sample compared to the TiO_2 sample. The narrower band gap is responsible for excitation of an electron from the valence band to the conduction band in N-TiO_2 and thus increases the photocatalytic activity of the material.

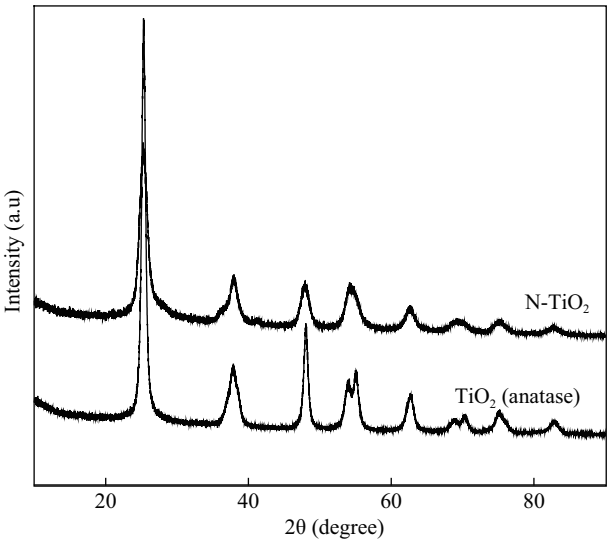

Fig. 1 XRD patterns of N-TiO_2.

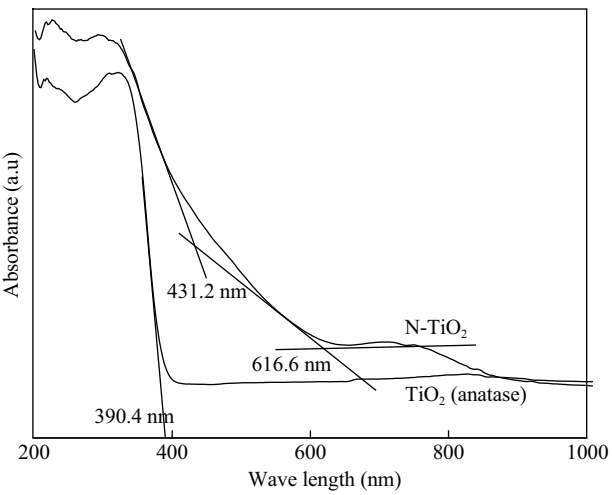

Fig. 2 UV-Vis diffuse reflectance spectra of N-TiO_2.

The TEM image of the N-TiO_2 is shown in **Fig. 3**. It can be seen that the crystallites agglomerated to larger particles. The images reveal that the sample consists of agglomerates of primary particles with the crystallite size ranging from about 6 to 10 nm which is in good agreement with the crystallite size calculated from XRD pattern. The diffraction patterns show the characteristics lines of anatase phase of TiO_2, which is in agreement with the XRD analysis.

The BET surface area of the sample was measured to be 176 m^2/g, the BET surface area of the TiO_2 (anatase) is 150 m^2/g.

Figure 4 shows XPS spectra of N1s electron with binding peak at the binding energy of 400 eV. The N concentration in the sample is about 0.20%. From the XPS results of different groups it has been observed that there is no consensus on the assignment of the N1s binding energy for nitrogen doped TiO_2. Generally there are two kinds of XPS peak observed in N-doped TiO_2. One with its binding energy around 397 eV is considered to be originating from nitrogen in Ti–N bond due to its proximity to the typical binding energy of Ti–N at 397.2 eV (Saha and Tomkins, 1992). The other with higher binding energy near 400 eV has been assigned by different groups to N1s in O-Ti-N environment. Satish et al. (2005) attributed a peak at 398.2 eV to N^- anion incorporated in the TiO_2 as N-Ti-O structural feature. Li et al. (2009) also attributed the peak at binding energy 398.6 eV to the N1s electron in N-Ti-O structure. Cong et al. (2007) observed two kinds of N-species with their binding energies 399.2 and 401.2 eV which were assigned to N-Ti-O and Ti-O-N linkages respectively. In their N-doped TiO_2 samples, Liu et al. (2009) observed peaks in the range 399.6 to 399.9 eV and attributed them to N-Ti-O form of nitrogen. Chen and Burda (2004), on the other hand, attributed the peak at 401.3 eV to nitrogen in the N-Ti-O environment. Thus different groups attributed different binding energies to N1s in N-Ti-O environment. The variation may be due to different preparation procedures adopted by the different groups. The N1s binding energy is higher when formal charge of N is more positive (Chen and Burda, 2004). When nitrogen forms N-Ti-O linkage, the electron density

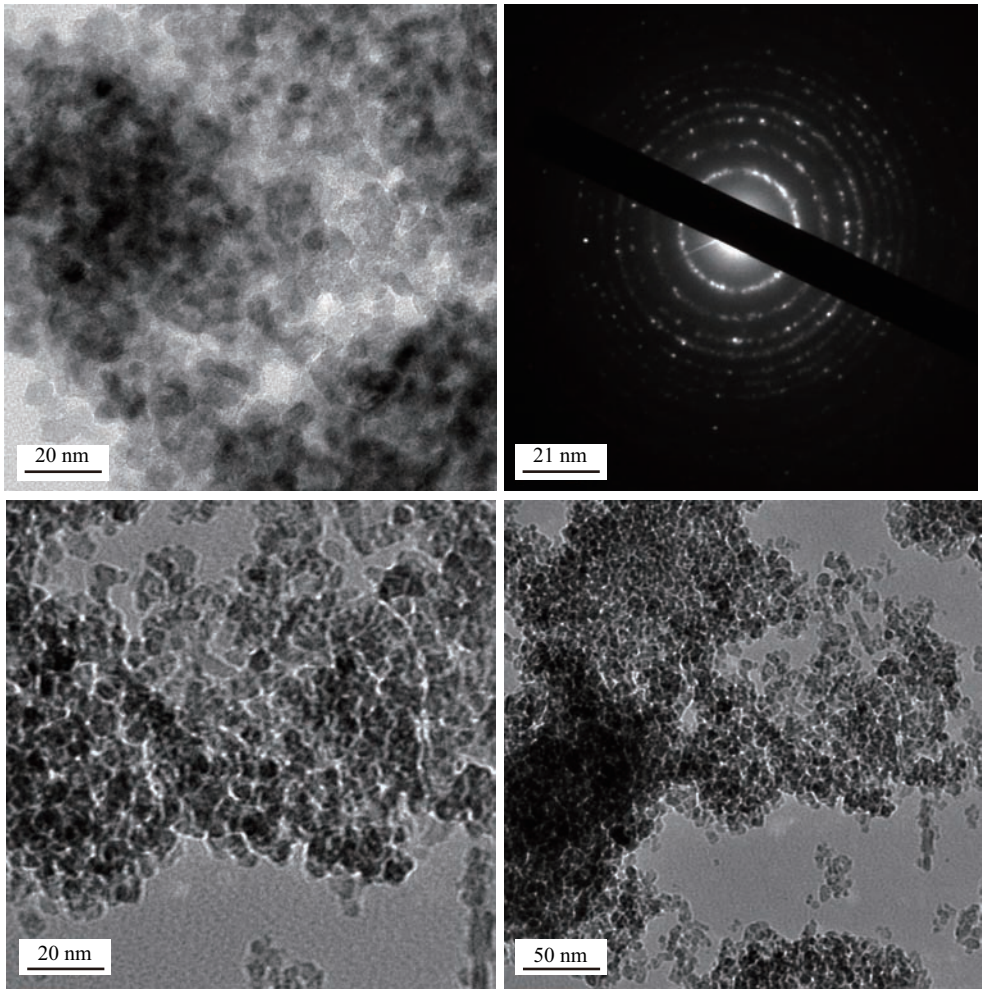

Fig. 3 TEM image of N-TiO_2 at different magnification.

around the nitrogen atom decreases compared to that in N-Ti-N of TiN because of the O atom. Thus, the N1s binding energy in N-Ti-O is higher than that in N-Ti-N. On the basis of above discussion we think the N1s binding energy peak at 400 eV in our sample is most probably due to O-Ti-N environment.

2.2 Adsorption capacity of Acid Blue 25 on N-TiO_2

2.2.1 Influence factors

The influence of amount of N-TiO_2 on the adsorption of Acid Blue 25 has been studied. For any fixed dose of N-TiO_2, the uptake increases and attains equilibrium within 60 min. At equilibrium (initial dye concentration 18 μmol/L), the adsorption increases from 7.1% to 34.4% for N-TiO_2 dose of 0.25 g/L to 1.0 g/L. The higher amounts of titania provide more surface for the dye to get adsorbed on it. However, further increase of adsorbent dose (1.5 g/L) decreases the extent of adsorption which may be due to particle agglomeration. **Figure 5a** represents the C_t/C_0 vs. t plots for different doses of N-TiO_2.

The initial dye concentration was studied by increasing the initial concentration of dye from 18.0 to 36.0 μmol/L,

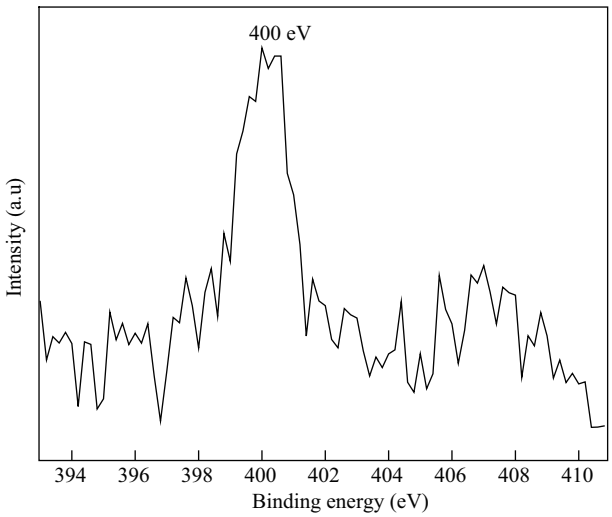

Fig. 4 XPS spectra of N-TiO_2.

the extent of adsorption varies from 10.5% to 13.2%. The initial higher uptake has been observed for first 10 min and equilibrium is attained within 60 min for all the cases (**Fig. 5b**).

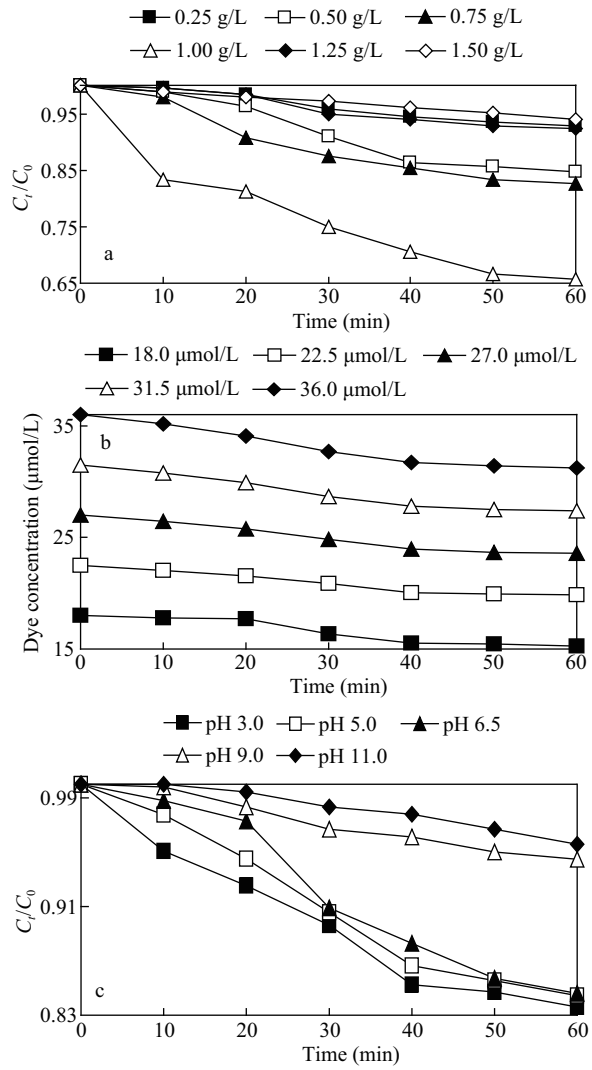

Fig. 5 Influence of N-TiO_2 dose (a), initial Acid Blue 25 concentration (b) and solution pH (c) on the adsorption of dye on N-TiO_2 at 303 K.

The pH of the aqueous solution is a significant controlling factor in adsorption mechanism. For 1.0 g/L of N-TiO_2 and initial dye concentration of 18 μmol/L, the extent of adsorption is maximum (16.3%) at pH 3.0 and showed a steady decrease upto pH 9.0 (4.0%) (**Fig. 5c**). At acidic pH, a significantly high electrostatic attraction exists between the positively charged surface of the N-TiO_2 and the anionic dye. As the pH of the system increases, the surface charge turns towards negative and adsorption of dye anions comes down (Bulut et al., 2008). Moreover, at high pH, there may be competition between OH^- and coloured ions of Acid Blue 25 for negatively charged adsorption sites on the surface of the adsorbent and the highly mobile OH^- ions are likely to be preferentially adsorbed in comparison to the bulky dye anions.

2.2.2 Adsorption isotherms

The adsorption of the dye on the pure and N doped TiO_2 has been studied by the well known Langmuir isotherm given by (Langmuir, 1918):

$$C_e/q_e = (1/bq_m) + (1/q_m)C_e \quad (2)$$

where, C_e and q_e are the concentration of dye and amount of dye adsorbed per unit mass of adsorbent at equilibrium respectively, q_m is the Langmuir monolayer adsorption capacity. The linear Langmuir plots are obtained by plotting C_e/q_e vs. C_e. The q_m values are calculated as 2.55×10^{-4} and 1.30×10^{-3} mg/g for pure and modified TiO_2, respectively.

2.2.3 Adsorption kinetics

The adsorption of Acid Blue 25 is studied by using Lagergren pseudo first-order model (Lagergren, 1898; Ho, 2004):

$$\log(q_e - q_t) = \log q_e - k_1 t \quad (3)$$

where, q_e and q_t are the amounts adsorbed per unit mass at equilibrium and at any time t, k_1 is the first order adsorption rate constant. For different doses of N-TiO_2, the log (q_e – q_t) vs. t plots (**Fig. 6a**) are linear (r: 0.885–0.991) and the first order rate constants (obtained from the slopes) varies from 6.12×10^{-2} to 7.48×10^{-2} min^{-1} for N-TiO_2 dose. Similarly, the k_1 values are in the range of 6.31×10^{-2} to 10.36×10^{-2} min^{-1} (r: 0.926~–0.969) for the variation of initial dye concentration from 18 to 36.0 μmol/L (**Fig. 6b**) and 6.60×10^{-2} to 3.33×10^{-2} min^{-1} as the solution pH changed from 3.0 to 11.0 (r: –0.957~–0.976) (**Fig. 6c**). All the k_1 values are listed in **Table 1**.

Table 1 Lagergren first order rate constants for adsorption of Acid Blue 25 on N-TiO_2

N-TiO_2 dose (g/L)	$k_1 \times 10^2$ (min^{-1})	Initial Acid Blue 25 conc. (μmol/L)	$k_1 \times 10^2$ (min^{-1})	pH	$k_1 \times 10^2$ (min^{-1})
0.25	6.12	18.0	6.31	3.0	6.60
0.50	6.31	22.5	8.47	5.0	6.58
0.75	7.16	27.0	8.54	6.5	6.31
1.00	7.48	31.5	8.72	9.0	5.46
1.25	5.91	36.0	10.36	11.0	3.33
1.50	3.73				

2.3 Photocatalytic decolourisation of Acid Blue 25 on N-TiO_2

2.3.1 Influence factors

Figure 7a shows the degradation profile of Acid Blue 25 with an initial concentration of 18 μmol/L under various catalyst loadings. The results reveal that the decolorizing efficiency shows increasing trend with the increase in N-TiO_2 loading from 0.25 to 1.25 g/L. The change in percentage decolourisation is maximum when catalyst amount is changed from 0.25 g/L (77.1% at 180 min)

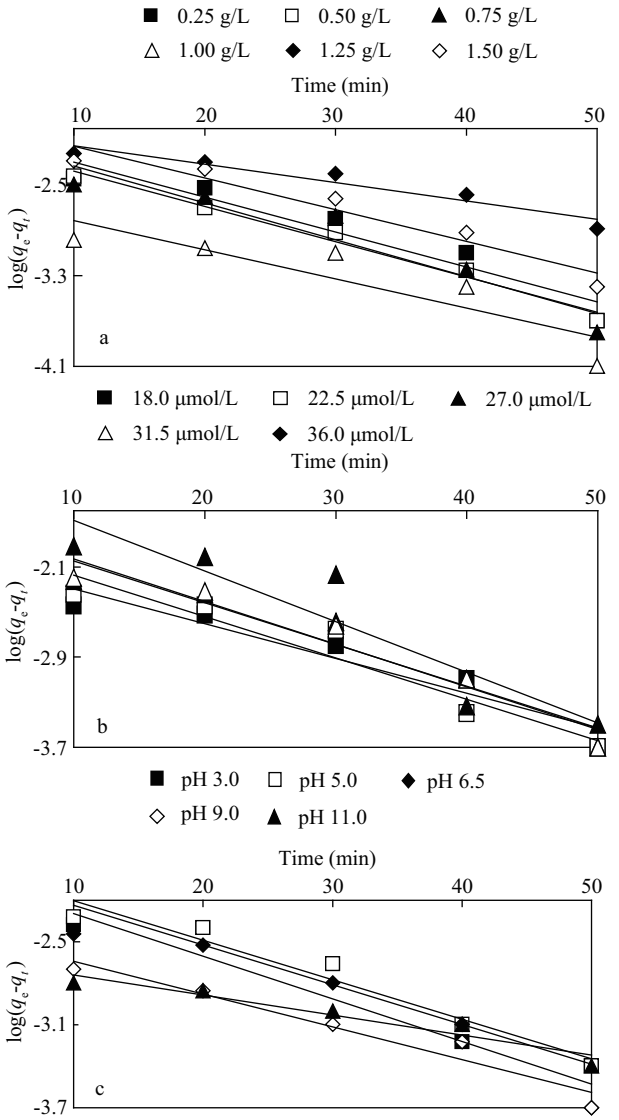

Fig. 6 Lagergren plots for adsorption of Acid Blue 25 on N-TiO_2 for the variation of N-TiO_2 dose (a), initial Acid Blue 25 concentration (b) and solution pH (c).

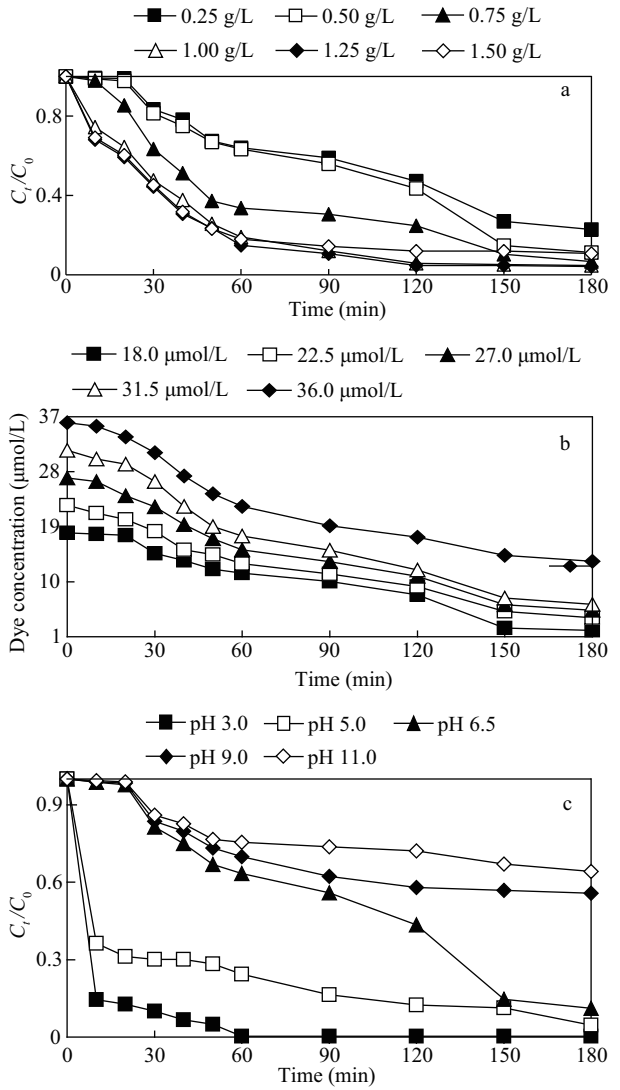

Fig. 7 Influence of N-TiO_2 dose (a), initial Acid Blue 25 concentration (b) and solution pH (c) on the decolourisation of dye on N-TiO_2 at 303 K.

to 0.5 g/L (88.8% at 180 min) compared to rest of the N-TiO_2 load (for 0.75 g/L: 89.9%, 1.0 g/L: 95.3%, 1.25 g/L: 95.8% (at 180 min)). However, the increase in N-TiO_2 loading above 1.25 g/L shows a decreasing trend in percentage decolourisation of Acid Blue 25 (for 1.5 g/L: 89.3% at 180 min). The increase of catalyst load beyond the optimum amount may result in the agglomeration of catalyst particles, and thus make a part of the catalyst surface become unavailable for light absorption, which lowers the efficiency of decolourisation (Huang et al., 2008). It has also been reported that as the excess catalyst prevent the illumination, concentration of OH radical, a primary oxidant in the photocatalytic system decreases which in turn decreases the efficiency of the dye decolourisation (Sun et al., 2008). Similar results were reported earlier (Nagaveni et al., 2004; Liu et al., 2006; Saquiba et al., 2008).

Figure 7b represents the effect of initial concentration of Acid Blue 25 on the decolourisation efficiency of N-TiO_2. For any concentration of the dye, rapid uptake takes place in the first 60 min and equilibrium was attained within 180 min. It can be seen from the **Fig. 7b** that the concentration has a significant effect on the degradation of dye.

The effect of solution pH on the efficiency of N-TiO_2 for decolourisation of Acid Blue 25 has been studied in the pH range of 3.0 to 11.0 (**Fig. 7c**). The study reveals that the extent of decolourisation increases with decrease in pH. At pH 3.0, 0.5 g/L N-TiO_2 can decolourise almost 100% Acid Blue 25 (initial concentration 18 μmol/L) within 60 min. It has been reported that acid-base properties of the metal oxide surfaces can have considerable implications upon their photocatalytic activity (Bahnemann et al., 1994). The formation of the electrical double layer at the solid-electrolyte interface affects the sorption-desorption processes and thus separate the photogenerated electron-

hole pairs at the surface of the semiconductor particles. Acid Blue 25 is an anionic dye having a sulphonate group and its adsorption is favoured at low pH (Sleiman et al., 2007) which may help the decolourisation reaction. Similar results were reported by other authors as well (Sleiman et al., 2007; Zhiyon et al., 2007).

2.3.2 Kinetics of photocatalytic degradation

The kinetics of the Acid Blue 25 decolorisation has been studied by modified Langmuir-Hinselwood (L-H) mechanism, given by Eq. (4):

$$-\mathrm{d}c/\mathrm{d}t = (kK_eC)/(1 + K_eC) \quad (4)$$

where, C is the concentration of dye, k (min^{-1}) is the apparent reaction rate constant, K_e is the apparent equilibrium constant for the adsorption of the dye on the catalyst surface.

Eq. (4) can be written as:

$$t = 1/(K_ek)\ln(C_0/C) + (1/k)(C_0 - C) \quad (5)$$

For the sufficient low concentration of dye, Eq. (5) can be expressed as:

$$\ln(C_0/C) = kK_et = k't \quad (6)$$

where, k' (min^{-1}) is the overall rate constant. By plotting $\ln(C_0/C)$ as a function of irradiation time through regression, we obtained for each catalyst sample the k' (min^{-1}) constant from the slopes.

The overall rate constant for Acid Blue 25 decolourisation on N-TiO_2 has been studied for the variation of catalyst load, initial dye concentration and solution pH. All the plots can be roughly considered as straight line (**Fig. 8**). The rate constants increase from 8.6×10^{-3} min^{-1} (catalyst load 0.25 g/L) to 17.8×10^{-3} min^{-1} (catalyst load 1.25 g/L) and then decrease to 10.9×10^{-3} min^{-1} for N-TiO_2 of 1.50 g/L, which indicates that the decolourisation rates depend on the catalyst amount. For different dye concentrations, the rate constant varies from 12.6×10^{-3} to 6.2×10^{-3} min^{-1} as the concentration of Acid Blue 25 changes from 18.0 to 36.0 μmol/L, which is consistent with the influence of variation of dye concentration on photocatalytic decolourisation. Similarly, the overall rate constant calculated at different pH are: $k'_{\mathrm{pH}\,3.0}$ (64.5×10^{-3}) > $k'_{\mathrm{pH}\,5.0}$ (13.1×10^{-3}) > $k'_{\mathrm{pH}\,6.5}$ (12.6×10^{-3}) > $k'_{\mathrm{pH}\,9.0}$ (3.5×10^{-3}) > $k'_{\mathrm{pH}\,11.0}$ (2.3×10^{-3}), which indicates that the decolourisation rate are pH dependent and lower pH favours the process more efficiently. All the values of degradation rate are given in the **Table 2**.

2.4 Comparison of decolourisation of Acid Blue 25 on N-TiO_2 with that of pure TiO_2 (anatase)

The decolourisation of Acid Blue 25 by N-TiO_2 has been compared with pure TiO_2 (anatase) (**Fig. 9**). It is found that, at 180 min (initial dye concentration: 18 μmol/L), 0.5 g/L of N-TiO_2 can decolourise 88.8% of Acid Blue 25 whereas only 12.7% dye decolourisation is done by TiO_2

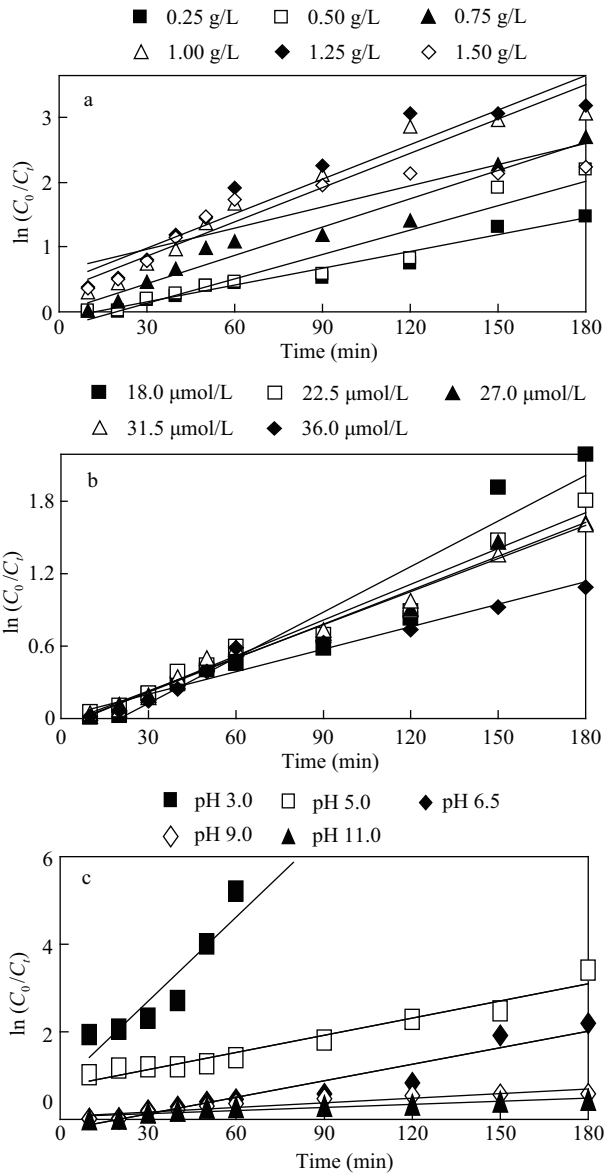

Fig. 8 Langmuir-Hinselwood plots for Acid Blue 25 degradation on N-TiO_2 for the variation of N-TiO_2 dose (a), initial acid blue concentration (b) and solution pH (c).

Table 2 Langmuir-Hiselwood first order rate constants for adsorption of Acid Blue 25 on N-TiO_2

N-TiO_2 dose (g/L)	k' ($\times 10^3$ min^{-1})	Initial Acid Blue 25 conc. (μmol/L)	$k' \times 10^3$ (min^{-1})	pH	$k' \times 10^{-3}$ (min^{-1})
0.25	8.6	18.0	12.6	3.0	64.5
0.50	12.6	22.5	9.9	5.0	13.1
0.75	14.5	27.0	9.4	6.5	12.6
1.00	17.6	31.5	9.1	9.0	3.5
1.25	17.8	36.0	6.2	11.0	2.3
1.50	10.9				

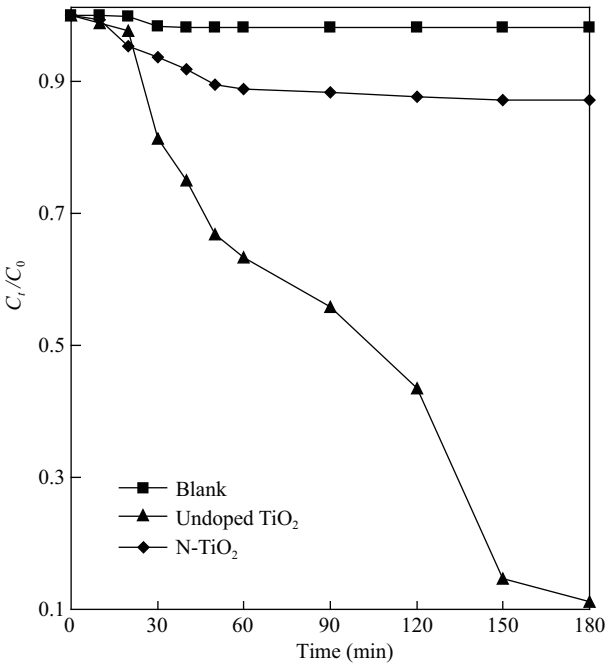

Fig. 9 Comparison of the photocatalytic degradation of Acid Blue 25 by undoped TiO_2 and N-TiO_2. Initial concentration of dye 18.0 μmol/L, catalyst load 1.0 g/L, temperature 300 K.

(under similar conditions). Thus, the modified TiO_2 can decolourise Acid Blue 25 almost 7 times more than pure TiO_2 (anatase). The blank experiment that has been carried out with the dye in absence of catalyst under visible light, reveals that a very negligible amount of decolourisation (2.2 %) has occurred (**Fig. 9**).

It is also found that the Langmuir-Hinselwood rate constant of Acid Blue 25 decolourisation by N-TiO_2 is ca. 21 times higher compared to the rate constant of the dye decolourisation by undoped TiO_2 under similar experimental conditions (k' for N-TiO_2: 12.6×10^{-3} min^{-1}; TiO_2: 6.0×10^{-4} min^{-1}).

3 Conclusions

Acid Blue 25 can be efficiently decolourised by visible light photocatalysis with nitrogen doped titania. The nitrogen doped nanocrystalline titania synthesized by a very simple method using $TiCl_3$ and aqueous NH_3 shows greater absorption of visible radiation and a red shift in the band gap energy compared to pure anatase TiO_2. The doped TiO_2 contains nitrogen in N-Ti-O environment. Both adsorption as well as photocatalytic decolourisation of Acid Blue 25 has been influenced by experimental variables, namely, N-TiO_2 dose, initial dye concentration and solution pH. The decoulorization efficiency increases with the increase in N-TiO_2 load from 0.25 to 1.25 g/L and then again decreases when the load is 1.5 g/L. The decrease of solution pH increases the decolourisation of dye and at pH 3.0, almost 100% Acid Blue 25 is decolourised (0.5 g/L N-TiO_2, initial concentration 18 μmol/L) within 60 min.

The modification of TiO_2 improved the decolourisation compared to pure TiO_2 (anatase) as the N-TiO_2 decolourised the dye almost 7 times more compared to undoped TiO_2. The higher visible light photo-catalytic activity of N-TiO_2 is possibly due to the fact that nitrogen doping effectively inhibits the recombination of the electron and the holes. Besides the higher absorption in the visible-light range and a red shift in the band gap indicates that more photoinduced electrons and holes could participate in the photocatalytic reactions in N-TiO_2 compared to TiO_2. The kinetics of dye decolourisation closely follows modified Langmuir-Hinshelwood (L-H) mechanism.

Acknowledgments

The authors are thankful to U.G.C, New Delhi for a Major Research Project grant. Authors are also thankful to Dr. C. V. V. Satyanarayana, Scientist, Catalysis Division, N. C. L., Pune, Prof. K. G. Bhattacharyya and Prof. J. N. Ganguli, Department of Chemistry, Gauhati University, Principal, B. N. College, Dhubri, Sri Goutam Kumar Sarma, Sri D. K. Kashyap for their help in various stages of this work.

References

Ao Y H, Xu J J, Fu D G, Yuan C W, 2009. Visible-light responsive C, N-codoped titania hollow spheres for X-3B dye photodegradation. *Microporous and Mesoporous Materials*, 118(1-3): 382–386.

Asahi R, Morikawa T, Ohwaki T, Aoki K, Taga Y, 2001. Visible-light photocatalysis in nitrogen-doped titanium oxides. *Science*, 293(5528): 269–271.

Bahnemann D W, Cunningham J, Fox M A, Pelizzetti E, Pichat P, Serpone N, 1994. "Photocatalytic Treatment of Waters" In: Aquatic Surface Photochemistry (Zepp R G, Heltz G R, Crosby D G, eds.). Lewis Publishers, Boca Raton. 261.

Bhatnagar A, Kumar E, Minocha A K, Jeon B H, Song H, Seo Y C, 2009. Removal of anionic dyes from water using citrus limonum (lemon) peel: equilibrium studies and kinetic modelling. *Separation Science and Technology*, 44(2): 316–334.

Bidaye P P, Khushalani D, Fernandes J B, 2009. A simple method for synthesis of S-doped TiO_2 of high photocatalytic activity. *Catalysis Letter*, 134(1-2): 169–174.

Bulut E, Özacar M, şengil I A, 2008. Equilibrium and kinetic data and process design for adsorption of congo red onto bentonite. *Journal of Hazardous Materials*, 154(1-3): 613–622.

Burda C, Lou Y, Chen X, Samia A C S, Stout J, Gole J L, 2003. Enhanced nitrogen doping in TiO_2 nanoparticles. *Nano Letters*, 3(8): 1049–1051.

Chen X B, Burda C C, 2004. Photoelectron spectroscopic investigation of nitrogen-doped titania nanoparticles. *Journal of Physical Chemistry B*, 108(40): 15446–15449.

Chi B, Zhao L, Jin T, 2007. One-step template-free route for synthesis of mesoporous N-doped titania spheres. *Journal of Physical Chemistry C*, 111(17): 6189–6193.

Cong Y, Zhang J, Chen F, Anpo M, 2007. Synthesis and characterization of nitrogen-doped TiO_2 nanophotocatalyst with high visible light activity. *Journal of Physical Chemistry C*, 111(19): 6976–6982.

Diwald O, Thompson T L, Zubkov T, Goralski E G, Walck S D, Yates J T Jr, 2004. Photochemical activity of nitrogen-doped rutile TiO_2(110) in visible light. *Journal of Physical Chemistry B*, 108(19): 6004–6008.

Du Z P, Feng C B, Li Q X, Zhao Y H, Tai X M, 2008. Photodegradation of NPE-10 surfactant by Au-doped nano-TiO_2. *Colloid and Surfaces A: Physicochemical and Engineering Aspects*, 315(1-3): 254–258.

Fu F, Gao Z W, Gao L X, Li D S, 2011. Effective adsorption of anionic dye, alizarin red S, from aqueous solutions on activated clay modified by iron oxide. *Industrial Engineering Chemistry Research*, 50(16): 9712–9717.

Gandhe A R, Fernandes J B, 2005. A simple method to synthesize visible light active N-doped anatase (TiO_2) photocatalyst. *Bulletin of Catalysis Society of India*, 4: 131–134.

Ghicov A, Macak J M, Tsuchiya H, Kunze J, Haeublein V, Frey L et al., 2006. Ion implantation and annealing for an efficient N-doping of TiO_2 nanotubes. *Nano Letters*, 6(5): 1080–1082.

Ghodbane H, Hamdaoui O, 2009. Intensification of sonochemical decolorization of anthraquinonic dye Acid Blue 25 using carbon tetrachloride. *Ultrasonics Sonochemistry*, 16(4): 455–461.

He C, Shu D, Su M H, Xia D H, Asi M A, Lin L et al., 2010. Photocatalytic activity of metal (Pt, Ag, and Cu)-deposited TiO_2 photoelectrodes for degradation of organic pollutants in aqueous solution. *Desalination*, 253(1-3): 88–93.

Ho Y S, 2004. Citation review of Lagergren kinetic rate equation on adsorption reactions. *Scientometrics*, 59(1): 171–177.

Huang M L, Xu C F, Wu Z B, Huang Y F, Lin J M, Wu J H, 2008. Photocatalytic discolorization of methyl orange solution by Pt modified TiO_2 loaded on natural zeolite. *Dyes and Pigments*, 77(2): 327–334.

Irie H, Watanabe Y, Hashimoto K, 2003. Nitrogen-concentration dependence on photocatalytic activity of $TiO_{2-x}N_x$ powders, *Journal of Physical Chemistry B*, 107(23): 5483–5486.

Kemp T J, Mclntyre R A, 2006. Transition metal-doped titanium(IV) dioxide: Characterisation and influence on photodegradation of poly(vinyl chloride). *Polymer Degradation Stability*, 91(1): 165–194.

Lagergren S, 1898. Zur theorie der sogenannten adsorption gelöster stoffe, Kungliga Svenska Vetenskapsakademiens. *Handlingar*, 24(4): 1–39.

Langmuir I, 1918. The adsorption of gases on plane surfaces of glass, mica, and platinum. *Journal of American Chemical Society*, 40(9): 1361–1403.

Li G S, Yu J C, Zhang D Q, Hu X L, Lau W M, 2009. A mesoporous $TiO_{2-x}N_x$ photocatalyst prepared by sonication pretreatment and *in situ* pyrolysis. *Separation and Purification Technology*, 67(2): 152–157.

Li Z J, Shen W Z, He W S, Zu X Z, 2008. Effect of Fe-doped TiO_2 nanoparticle derived from modified hydrothermal process on the photocatalytic degradation performance on methylene blue. *Journal of Hazardous Materials*, 155(3): 590–594.

Lin J, Lin Y, Liu P, Meziani M J, Allard L F, Sun Y P, 2002. Hot-fluid annealing for crystalline titanium dioxide nanoparticles in stable suspension. *Journal of the American Chemical Society*, 124(38): 11514–11518.

Liu G, Wang X W, Chen Z G, Cheng H-M, Lu G Q M, 2009. The role of crystal phase in determining photocatalytic activity of nitrogen doped TiO_2. *Journal of Colloid and Interface Science*, 329(2): 331–338.

Liu J W, Han R, Zhao Y, Wang H T, Lu W J, Yu T F et al., 2011. Enhanced photoactivity of V-N codoped TiO_2 derived from a two-step hydrothermal procedure for the degradation of PCP-Na under visible light irradiation. *Journal of Physical Chemistry C*, 115(11): 4507–4515.

Liu S, Yang J H, Choy J H, 2006. Microporous SiO_2-TiO_2 nanosols pillared montmorillonite for photocatalytic decomposition of methyl orange. *Journal of Photochemistry and Photobiology A: Chemistry*, 179(1-2): 75–80.

Livraghi S, Paganini C, Giamello E, Selloni A, Valentin C D, Pacchioni G, 2006. Origin of photoactivity of nitrogen-doped titanium dioxide under visible light. *Journal of the American Chemical Society*, 128(49): 15666–15671.

Ma Y, Fu J W, Tao X, Li X, Chen J F, 2011. Low temperature synthesis of iodine-doped TiO_2 nanocrystallites with enhanced visible-induced photocatalytic activity. *Applied Surface Science*, 257(11): 5046–5051.

Mwabora J M, Lindgren T, Avendaño E, Jaramillo T F, Lu J, Lindquist S-E et al., 2004. Structure, composition, and morphology of photoelectrochemically active $TiO_{2-x}N_x$ thin films deposited by reactive DC magnetron sputtering. *The Journal of Physical Chemistry B*, 108(52): 20193–20198.

Nagaveni K, Sivalingam G, Hegde M S, Madras G, 2004. Solar photocatalytic degradation of dyes: high activity of combustion synthesized nano TiO_2. *Applied Catalysis B: Environmental*, 48(2): 83–93.

Narayan H, Alemu H, Macheli L, Sekota M, Thakurdesai M, Gundu Rao T K, 2009. Role of particle size in visible light photocatalysis of congo red using TiO_2. $[ZnFe_2O_4]_x$ nanocomposites. *Bulletin of Material Science*, 32(5): 499–506.

Saha N C, Tomkins H C J, 1992. Titanium nitride oxidation chemistry: an X-ray photoelectron spectroscopy study. *Journal of Applied Physics*, 72(7): 3072–3079.

Sakthivel S, Janczarek M, Kisch H, 2004. Visible light activity and photoelectrochemical properties of nitrogen-doped TiO_2. *The Journal of Physical Chemistry B*, 108(50): 19384–19387.

Saquiba M, Tariqa M A, Faisala M, Muneer M, 2008. Photocatalytic degradation of two selected dye derivatives in aqueous suspensions of titanium dioxide. *Desalination*, 219(1-3): 301–311.

Sathish M, Viswanathan B, Viswanath R P, Gopinath C S, 2005. Synthesis, characterization, electronic structure, and photocatalytic activity of nitrogen-doped TiO_2 nanocatalyst. *Chemistry of Materials*, 17(25): 6349–6353.

Sato S, Nakamura R, Abe S, 2005. Visible-light sensitization of TiO_2 photocatalysts by wet-method N-doping. *Applied Catalysis A: General*, 284(1-2): 131–137.

Shao G S, Zhang X J, Yuan Z Y, 2008. Preparation and photocatalytic activity of hierarchically mesoporous-macroporous $TiO_{2-x}N_x$. *Applied Catalysis B: Environmental*, 82(3-4):

208–218.

Silveyra R, Sáenz L D L T, Flores W A, Martínez V C, Elguézabal A A, 2005. Doping of TiO_2 with nitrogen to modify the interval of photocatalytic activation towards visible radiation. *Catalysis Today*, 107-108: 602–605.

Sleiman M, Vildozo D, Ferronato C, Chovelon J M, 2007. Photocatalytic degradation of azo dye metanil yellow: optimization and kinetic modeling using a chemometric approach. *Applied Catalysis B: Environmental*, 77(1-2): 1–11.

Sobana N, Selvam K, Swaminathan M, 2008. Optimization of photocatalytic degradation conditions of direct red 23 using nano-Ag doped TiO_2. *Separation and Purification Technology*, 62(3): 648–653.

Sun J H, Qiao L P, Sun S P, Wang G L, 2008. Photocatalytic degradation of orange G on nitrogen-doped TiO_2 catalysts under visible light and sunlight irradiation. *Journal of Hazardous Materials*, 155(1-2): 312–319.

Tachikawa T, Tojo S, Kawai K, Endo M, Fujitsuka M, Ohno T et al., 2004. Photocatalytic oxidation reactivity of holes in the sulfur- and carbon-doped TiO_2 powders studied by time-resolved diffuse reflectance spectroscopy. *Journal of Physical Chemistry*, 108(50): 19299-19306.

Valentin C D, Pacchioni G, Selloni A, Livraghi S, Giamello E, 2005. Characterization of paramagnetic species in N-doped TiO_2 powders by EPR spectroscopy and DFT calculations. *The Journal of Physical Chemistry B*, 109(23): 11414–11419.

Wang X P, Lim T T, 2010. Solvothermal synthesis of C-N codoped TiO_2 and photocatalytic evaluation for bisphenol A degradation using a visible-light irradiated LED photoreactor. *Applied Catalysis B: Environmental*, 100(1-2): 355–364.

Wang Y Q, Yu X J, Sun D Z, 2007. Synthesis, characterization, and photocatalytic activity of $TiO_{2-x}N_x$ nanocatalyst. *Journal of Hazardous Materials*, 144(1-2): 328–333.

Wang Y Y, Zhou G W, Li T D, Qiao W T, Li Y J, 2009. Catalytic activity of mesoporous $TiO_{2-x}N_x$ photocatalysts for the decomposition of methyl orange under solar simulated light. *Catalysis Communication*, 10(4): 412–415.

Wu Y, Xing M, Zhang J, 2011. Gel-hydrothermal synthesis of carbon and boron co-doped TiO_2 and evaluating its photocatalytic activity. *Journal of Hazardous Materials*, 192(1): 368–373.

Xing M Y, Zhang J H, Chen F, 2009. New approaches to prepare nitrogen-doped TiO_2 photocatalysts and study on their photocatalytic activities in visible light. *Applied Catalysis B: Environmental*, 89(3-4): 563–569.

Xu J J, Ao Y H, Fu D G, Yuan C H, 2008. Low-temperature preparation of F-doped TiO_2 film and its photocatalytic activity under solar light. *Applied Surface Science*, 254(10): 3033–3038.

Yin S, Aita Y, Komatsu M, Wang J S, Tang Q, Sato T, 2005. Synthesis of excellent visible-light responsive $TiO_{2-x}N_y$ photocatalyst by a homogeneous precipitation-solvothermal process. *Journal of Material Chemistry*, 15(6): 674–682.

Yu J C, Ho W, Yu J, Yip H, Wong P K, Zhao J, 2005. Efficient visible-light-induced photocatalytic disinfection on sulfur-doped nanocrystalline titania. *Environmental Science & Technology*, 39(4): 1175–1179.

Yu Z Y, Bensimon M, Sarria V, Stolitchnov I, Jardim W, Laub D et al., 2007. $ZnSO_4$-TiO_2 doped catalyst with higher activity in photocatalytic processes. *Applied Catalysis B: Environmental*, 76(1-2): 185–195.

Zhang Z B, Wang C C, Zakaria R, Ying J Y, 1998. Role of particle size in nanocrystalline TiO_2-based photocatalysts. *Journal of Physical Chemistry B*, 102(52): 10871–10878.

Zhu J F, Deng Z G, Chen F, Zhang J L, Chen H J, Anpo M et al., 2006. Hydrothermal doping method for preparation of Cr^{3+}-TiO_2 photocatalysts with concentration gradient distribution of Cr^{3+}. *Applied Catalysis B: Environmental*, 62(3-4): 329–335.

JOURNAL OF ENVIRONMENTAL SCIENCES

环境科学学报(英文版)

(http://www.jesc.ac.cn)

Aims and scope

Journal of Environmental Sciences is an international academic journal supervised by Research Center for Eco-Environmental Sciences, Chinese Academy of Sciences. The journal publishes original, peer-reviewed innovative research and valuable findings in environmental sciences. The types of articles published are research article, critical review, rapid communications, and special issues.

The scope of the journal embraces the treatment processes for natural groundwater, municipal, agricultural and industrial water and wastewaters; physical and chemical methods for limitation of pollutants emission into the atmospheric environment; chemical and biological and phytoremediation of contaminated soil; fate and transport of pollutants in environments; toxicological effects of terrorist chemical release on the natural environment and human health; development of environmental catalysts and materials.

For subscription to electronic edition

Elsevier is responsible for subscription of the journal. Please subscribe to the journal via http://www.elsevier.com/locate/jes.

For subscription to print edition

China: Please contact the customer service, Science Press, 16 Donghuangchenggen North Street, Beijing 100717, China. Tel: +86-10-64017032; E-mail: journal@mail.sciencep.com, or the local post office throughout China (domestic postcode: 2-580).

Outside China: Please order the journal from the Elsevier Customer Service Department at the Regional Sales Office nearest you.

Submission declaration

Submission of an article implies that the work described has not been published previously (except in the form of an abstract or as part of a published lecture or academic thesis), that it is not under consideration for publication elsewhere. The submission should be approved by all authors and tacitly or explicitly by the responsible authorities where the work was carried out. If the manuscript accepted, it will not be published elsewhere in the same form, in English or in any other language, including electronically without the written consent of the copyright-holder.

Submission declaration

Submission of the work described has not been published previously (except in the form of an abstract or as part of a published lecture or academic thesis), that it is not under consideration for publication elsewhere. The publication should be approved by all authors and tacitly or explicitly by the responsible authorities where the work was carried out. If the manuscript accepted, it will not be published elsewhere in the same form, in English or in any other language, including electronically without the written consent of the copyright-holder.

Editorial

Authors should submit manuscript online at http://www.jesc.ac.cn. In case of queries, please contact editorial office, Tel: +86-10-62920553, E-mail: jesc@263.net, jesc@rcees.ac.cn. Instruction to authors is available at http://www.jesc.ac.cn.

Journal of Environmental Sciences (Established in 1989)

Vol. 25 No. 5 2013

Supervised by	Chinese Academy of Sciences	**Published by**	Science Press, Beijing, China
Sponsored by	Research Center for Eco-Environmental		Elsevier Limited, The Netherlands
	Sciences, Chinese Academy of Sciences	**Distributed by**	
Edited by	Editorial Office of Journal of	Domestic	Science Press, 16 Donghuangchenggen
	Environmental Sciences		North Street, Beijing 100717, China
	P. O. Box 2871, Beijing 100085, China		Local Post Offices through China
	Tel: 86-10-62920553; http://www.jesc.ac.cn	Foreign	Elsevier Limited
	E-mail: jesc@263.net, jesc@rcees.ac.cn		http://www.elsevier.com/locate/jes
Editor-in-chief	Hongxiao Tang	**Printed by**	Beijing Beilin Printing House, 100083, China

CN 11-2629/X **Domestic postcode: 2-580** **Domestic price per issue RMB ¥ 110.00**

ISSN 1001-0742

9 771001 074130 05>